Bull Volcanol (2009) 71:1195–1208
DOI 10.1007/s00445-009-0294-6

RESEARCH ARTICLE

# Chronostratigraphy of Monte Vulture volcano (southern Italy): secondary mineral microtextures and $^{39}$Ar-$^{40}$Ar systematics

**Igor M. Villa · Annett Buettner**

Received: 17 May 2004 / Accepted: 7 May 2009 / Published online: 6 June 2009


**Abstract** The eruptive history of Monte Vulture has been the subject of several geochronological investigations during the past decades, which reliably dated only a small number of eruptions. Understanding the causes of sub-optimum data yield in the past requires an interdisciplinary approach. We re-analyzed samples from previous works and present new data on samples from the main volcano-stratigraphic units of Monte Vulture, so as to provide an improved, consistent chronostratigraphic database. Imaging of minerals by cathodoluminescence and backscattered electrons reveals that heterochemical, high-temperature deuteric reaction textures are ubiquitous. Such observations are common in metamorphic rocks but had not frequently been reported from volcanic rocks. In view of the mineralogical complexity, we base our chronological interpretation on isochemical steps, defined as steps for which the Cl/K and/or the Ca/K ratios are constant. Isochemical steps carry the isotopic signature of chemically homogeneous mineral phases and therefore allow a well-constrained age interpretation. Comparison of old and new $^{39}$Ar-$^{40}$Ar data proves the reproducibility of age spectra and their shapes. This quantifies the analytical reliability of the irradiation and mass-spectrometric analyses. Anomalous age spectra are a reproducible property of some specific samples and correlate with mineralogical anomalies. The present data allow us to fine-tune the age of the volcanostratigraphic units of Monte Vulture during the known interval of main volcanic activity from ca. 740 to 610 ka. After a very long stasis, the volcanic activity in the Monte Vulture area resumed with diatremic eruptions, one of which (Lago Piccolo di Monticchio, the site of a palynological-paleoclimatological drilling) was dated at ca. 140 ka.

**Keywords** $^{39}$Ar-$^{40}$Ar dating · Isochemical ages · Monte Vulture volcano · Deuteric reactions · Monticchio Lakes · Melfi haüynophyre · Campanian Ignimbrite

Editorial responsibility: R. Cioni

**Electronic supplementary material** The online version of this article (doi:10.1007/s00445-009-0294-6) contains supplementary material, which is available to authorized users.

I. M. Villa (✉) · A. Buettner
Institut für Geologie, Universität Bern,
Baltzerstrasse 3,
3012 Bern, Switzerland
e-mail: igor@geo.unibe.ch

I. M. Villa
Dipartimento di Scienze Geologiche e Geotecnologie,
Università di Milano Bicocca,
20126 Milano, Italy

*Present Address:*
A. Buettner
LPK GmbH,
Frankfurt, Germany

## Introduction

Monte Vulture is a Quaternary volcano in southern Italy. It is located to the east of the main Apenninic chain, on the Apulian platform. The dominant rock series range from basanite through tephrite and foidite to phonolite (Melluso et al. 1996); the latest eruptive products have been described as carbonatite-melilitites (Stoppa and Principe 1997). The variability and petrological features of its magmas are unique among Italian potassic volcanoes (De Astis et al. 2006). Their genesis is certainly complex and

exceeds the purpose of this paper (see, e.g., the review by Peccerillo 2005, and references therein).

Previous authors (e.g., La Volpe and Principe 1991, Stoppa and Principe 1997) divided the volcanic activity into several discrete cycles. Recent studies (Giannandrea et al. 2002; Principe and Giannandrea 2002) present a refined volcanostratigraphical profile and provide a detailed subdivision into units bounded by unconformities (synthems and subsynthems, Fig. 1). The Monte Vulture Supersynthem led to the build-up of a strato-volcano and was interrupted by an early caldera collapse that resulted in an overlapping of products emitted from different vents. Meter-thick dykes of this supersynthem intruded basement and are assigned to the Spinoritola Subsynthem. Two large eruptions led to the deposition of the Lower and Upper Ignimbrite, grouped in the Fara d'Olivo Subsynthem. The Barile Synthem is characterised by a subvolcanic body, the Toppo San Paolo dome, and repeated discrete explosive eruptions, which resulted in the cone-building phase. The main volcanic activity ends with the eruption of lavas and pyroclastics (Vulture San Michele Subsynthem) and with phreatomagmatic eruptions (Ventaruolo Subsynthem). A spatially isolated small lava flow of unique composition (Melfi haüynophyre: Hieke Merlin 1967) is assigned to the Melfi Synthem concluding the Monte Vulture Supersynthem. After a period of quiescence, the volcanic edifice became dismembered by normal faulting (Valle dei Greggi-Fosso del Corbo fault system); volcanism resumed as well with volumetrically subordinate eruptions assigned to the Laghi di Monticchio Supersynthem. The normal fault system caused subsidence of the southern half of the Vulture edifice (La Volpe and Principe 1991) and collapse of its SW portion (Principe and Giannandrea 2002). The Laghi di Monticchio Supersynthem is represented by deposits of scattered eruptive centres along the active fault systems (Principe and Giannandrea 2002). This led to the formation of diatremic structures, two of which are the Monticchio Lakes (Stoppa and Prinicipe 1997).

During the past three decades several authors have presented geochronological data: K-Ar analyses (Cortini 1975) and $^{39}$Ar-$^{40}$Ar analyses (Villa 1985, 1988, 1991; Brocchini et al. 1994; Bonadonna et al. 1998). The $^{39}$Ar-$^{40}$Ar studies broadly constrain the main volcanic activity of Monte Vulture, but show significant discrepancies.

Data presented in Brocchini et al. (1994) and Bonadonna et al. (1998) were calculated using an assumed age of 27.55 Ma for the Fish Canyon (FC) irradiation monitor; the Renne et al. (1998) calibration of FC, 28.02 Ma, results in an increase of ages by ca. 2%. Furthermore, ages published by Bonadonna et al. (1998) were expressed as isochron calculations. It should be noted that isochrons (correlation of $^{36}$Ar/$^{40}$Ar and $^{39}$Ar/$^{40}$Ar) mostly do not consider the possible presence of non-cogenetic phases in a mineral separate (Villa 1992). An alignment of data points alone does not guarantee that a single, monogenetic phase was analyzed (Villa 2001), and chemical correlation diagrams are required (see below). Here we recalculated nine ages of Brocchini et al. (1994) and Bonadonna et al. (1998) on the basis of the raw data in Brocchini (1993) and of the petrological-chemical criteria outlined below.

According to petrological investigations by De Fino et al. (1986), Vulture volcanics were often affected by interaction with high-temperature $H_2O$-rich and/or $CO_2$-rich fluids, at least in part already in the pre-eruptive stage. This interaction resulted in partial or complete transformation of primary mineral phases. Hence, most of the analyzed minerals

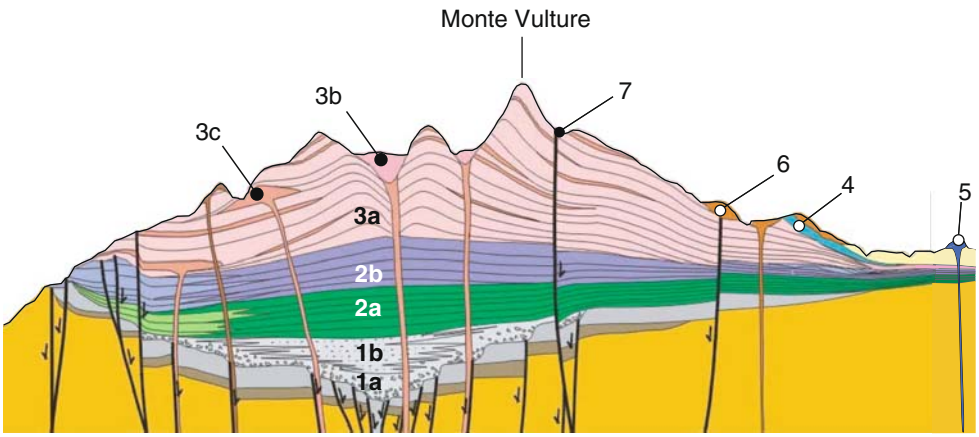


**Fig. 1** Geological cross section of Monte Vulture (redrawn after Giannandrea et al. 2002). Subsynthems of Monte Vulture Supersynthem: (1) Fara d'Olivo Subsynthem, (a) epiclastics, (b) tephra; (2) Rionero Subsynthem, (a) *Lower* series, (b) *Upper* series; (3) Vulture San Michele Subsynthem, (a) tephra, (b) lavas; (4) Ventaruolo Subsynthem; (5) Melfi Subsynthem. Subsynthems of Monticchio Supersynthem: (6) Case Lopes Subsynthem; (7) Lago Piccolo Subsynthem

(1) Fara d'Olivo Subsynthem, (a) epiclastics, (b) tephra; (2) Rionero Subsynthem, (a) Lower series, (b) Upper series; (3) Vulture San Michele Subsynthem, (a) tephra, (b) lavas; (4) Ventaruolo Subsynthem; (5) Melfi Subsynthem; (6) Case Lopes Subsynthem; (7) Lago Piccolo Subsynthem.

represent multiphase systems and are therefore likely to record perturbed $^{39}$Ar-$^{40}$Ar systematics. Additionally, Ar systematics can likewise be influenced by the complex processes that commonly impact on the generation of carbonatitic and melilitolitic magmas, which result in zonation and multistage phase generation (Di Muro et al. 2004). Finally, expansion of mineral lattices can occur during water-melt interaction, hydrothermal mineral alteration and/or weathering, causing cation exchange and, in particular, analcimization of leucite. Amongst the mineral modifications we described, these are the only ones that occurred at low temperature and at a time substantially later than emplacement; these samples are also easiest to discard, as the petrography of meteoric alteration has been studied for centuries.

We focus on these deuteric mineral heterogeneities and present a combination of mineralogical investigations and $^{39}$Ar-$^{40}$Ar analyses on different K-bearing phases to address the influence of mineral complexity on $^{39}$Ar-$^{40}$Ar systematics. Note that the implicit assumption of many geochronologists is that volcanic minerals are simple, ideal, "frozen" archives that flawlessly record the magma, its chemistry, and its age. Our observations instead are that in Vulture rocks heterochemical, mostly high-temperature, deuteric reaction textures are ubiquitous. Such observations are common in metamorphic rocks (e.g. Vance et al. 2003, and references therein); our work extends the database of such images also to volcanic rocks, and explicitly addresses the link between microtextures and isotopic record.

Five mineral separates analyzed in this study were remaining aliquots from previous investigations (VUT 110, 168, and 251; VU 1680 and 1813: Table A1 (electronic supplement)). A direct comparison with published data allows an assessment of external reproducibility. Our recognition of mixtures of pristine and deuterically modified mineral domains led us to a more rigorous choice of steps for regression relative to those published by previous authors (see the geochronology paragraph). We observe that in most cases this does not upset the estimated ages; we also observe a very tight reproducibility both amongst new and old sample preparations, and in the shape of the age spectra.

## Analytical techniques

Rocks were crushed and sieved; selected size fractions (100–150 μm up to 250–350 μm) were separated using magnetic and density techniques at the Istituto di Geocronologia facilities in Pisa during the 1980s. Additional ultrasonic cleaning and hand-picking was performed on the samples analyzed by us. Separates for the present work were irradiated at the McMasters Research Reactor (Canada) without Cd-shielding. FC sanidine with an assigned age of 28.02 Ma (Renne et al. 1998) was used as the irradiation monitor. The $^{39}$Ar-$^{40}$Ar analyses were performed on the MAP™ 215-50B noble-gas mass spectrometer in Berne using the incremental heating technique. A detailed description of the apparatus and of the interference corrections is given in Villa et al. (2000). All isotopes were measured on the Faraday collector. Two $^{39}$Ar-$^{40}$Ar analyses were performed at Istituto di Geocronologia e Geochimica Isotopica, CNR, Pisa (Villa unpublished data 1988) on a Varian MAT™ 240, equipped with a Baur-Signer source; only $^{40}$Ar, $^{39}$Ar and $^{36}$Ar were measured, all on an electron multiplier. The complete dataset of $^{39}$Ar-$^{40}$Ar analyses is given in Table A2 (electronic supplement); in Table A2 uncertainties are given as 1 standard deviation, while uncertainties on calculated ages discussed in the text are given as 2 standard deviations. Table A3 (electronic supplement) contains, for convenience, additional derived quantities calculated from the complete dataset in Table A2.

Cathodoluminescence (CL) images were acquired on both thin sections and single-grain mounts. A high-sensitivity CL microscope (Ramseyer et al. 1989) attached to a computer-controlled digital camera system (ColorView™ 12 run under analySIS™ FIVE image analysis program) was used to record the luminescence characteristics in the visible range of the electromagnetic spectrum. The applied beam current density was 0.2–0.4 μA/mm$^2$ at 25 keV electron energy. Back-scattered electron (BSE) imaging and element mapping were carried out using a Cameca SX-50 electron microprobe (EMP) with an acceleration voltage of 15 kV and a beam current of 50 nA. Both microbeam analytical facilities are located at Universität Bern. Typical mineral textures are shown in Fig. 2.

## Mineralogy

K-bearing phases, namely sanidine, leucite, biotite and phlogopite were separated from numerous volcanic units. Mineralogical and microchemical observations based on CL and BSE images provide an insight into compositional and crystallographic characteristics of these minerals. Element mapping provides quantitative information about the distribution of selected elements.

### Leucite

The leucites of Mt. Vulture are frequently deeply altered and replaced by turbid analcime (e.g. De Fino et al. 1986). Nearly euhedral, clear leucite crystals from sample VU 1907 (Vulture San Michele Subsynthem) were checked for their preservation and purity using EMP element mapping and CL images. The phenocrysts are chemically homogeneous and exhibit a uniform gray-shade (Fig. 2a) which

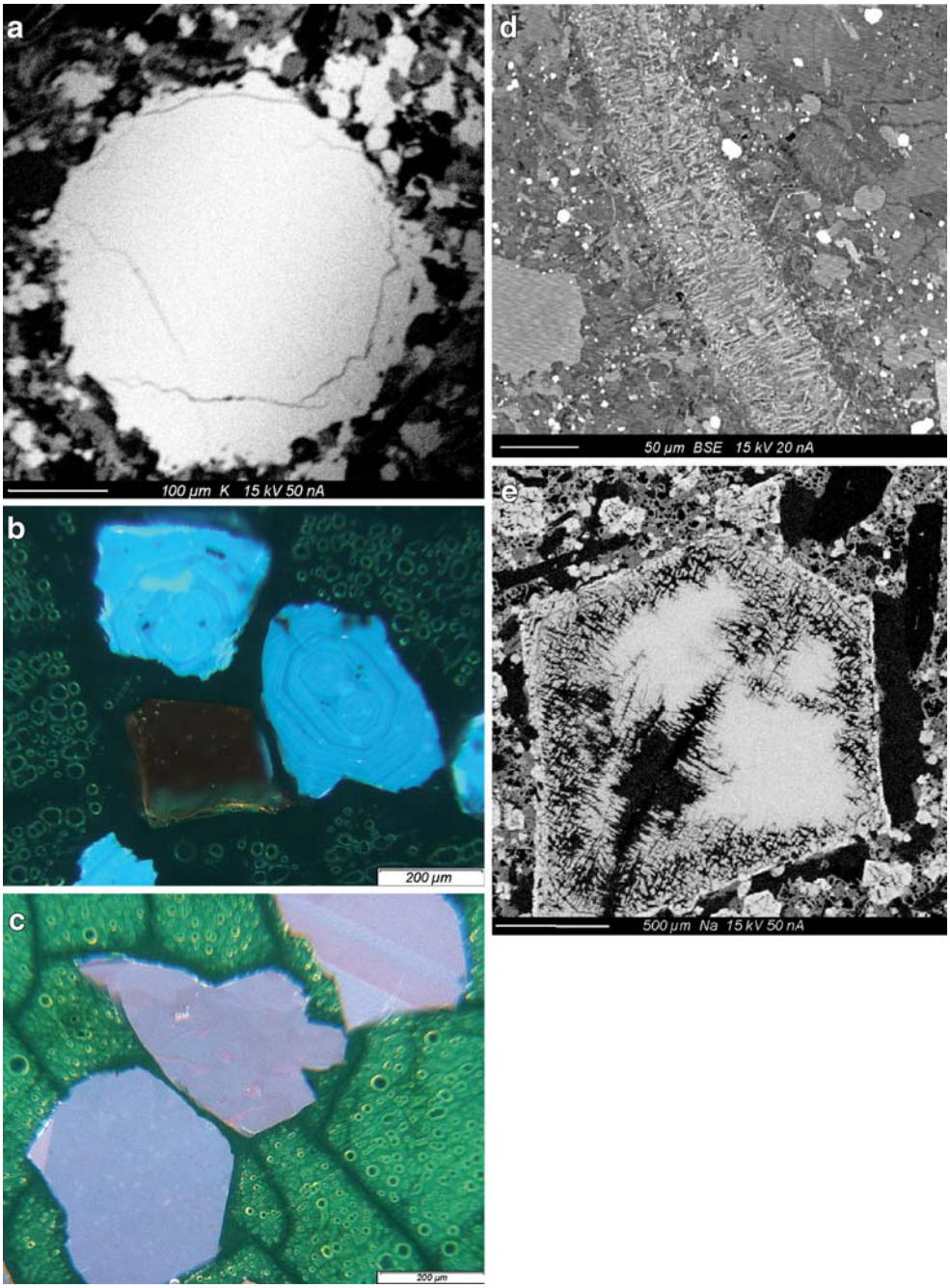


**Fig. 2** **a** Microchemical K element-mapping in leucite VU 1907. The homogenous light colour indicates an even K distribution over the crystal. Size of photo 0.5×0.5 mm. **b** Cathodoluminescence (CL) image of leucite grains (sample VU 1907). Crystals are characterised by zonations sometimes with disturbed growth pattern (right crystal with two cores). Size of photo 0.9×0.9 mm. **c** CL image of sanidine grains (sample VU 1680). Cloudy patches with colour variations in all three grains indicate chemical heterogeneity and possible alteration. Size of photo 0.9×0.9 mm. **d** Back-scattered electron image of biotite VUT 0001. Recrystallisation mica needles fill up the former shape of a coarse grained mica crystal. Size of photo 0.3×0.3 mm. **e** Microchemical Na element-mapping of noseane VU 1523. K behaves antithetically to Na. Inflow of K and loss of Na along a prominent crack and alkali exchange along a reaction front at the grain boundary attest to a multi-stage chemical exchange history. Size of photo 2×2 mm

corresponds to a uniform K distribution. They have a $K_2O$ content of 20 wt%, only slightly below the expected stoichiometric value of 21.6%. CL shows growth zonation of the crystals and sporadic blue patches (Fig. 2b); the latter might be related to the small stoichiometric disturbance. Ca and Cl were below the detection limit of ca. 100 ppm.

## Sanidine

Optical microscope observations of subhedral sanidines, embedded in a porous rock matrix, sometimes show mottled textures indicative for secondary reactions. $K_2O$ contents average around 13 wt% and only in one case (sample VUG 1) it is below 10 wt%. CL images of sanidine VU 1680 (Fig. 2c) reveal pink-purple patches that are a likely effect of a disturbance within the mineral structure (Ramseyer, pers. comm. 2004).

## Biotite

Biotite phenocrysts are brown to dark brown and generally subhedral. Biotites of sample VUT 0001 (Fig. 2d) show

tiny recrystallization needles pseudomorphing the original coarse-grained crystal. BSE images of some biotites analysed by $^{39}Ar$-$^{40}Ar$ show no obvious disturbances, but the $K_2O$ content is between 5 and 8 wt%, clearly non-stoichiometric. The presence of secondary phases such as chlorite is probably responsible for low $K_2O$ contents in all investigated samples. These phases are not visible in BSE images but an interlayering of biotite and chlorite has been shown to occur at the nm scale (Di Vincenzo et al. 2003), much below the spatial resolution of the EMP.

### Phlogopite

Phlogopite phenocrysts are ubiquitous and frequently associated with biotite. Some phlogopites exhibit Ti-enriched opaque reaction rims (Melluso et al. 1996). Calculated $K_2O$ contents of phlogopite range between 8 and 11 wt%, confirming the importance of secondary reactions in lowering the K concentration below stoichiometry.

### Noseane

The secondary reaction textures are especially spectacular in the case of noseane. The euhedral noseane phenocrysts from the Melfi haüynophyre are up to several mm in diameter and colourless (Fig. 2e). The comparison of Na and K element-mapping shows that K behaves antithetically to Na. De Fino et al. (1986) emphasize deep, high-temperature deuterization processes, with the possible involvement of $SO_4$. Accordingly, we propose that Na was replaced by K during secondary processes (Fig. 3).

### Mineralogy from Ar isotope systematics

Our mineralogical observations have documented that several samples consist of mixtures of mineral phases. In order to unravel the Ar systematics, one can apply three-isotope correlation plots such as described, e.g., by Villa (2001). Irradiation-produced isotopes $^{39}Ar$, $^{38}Ar$ and $^{37}Ar$ act as proxies for K, Cl and Ca, respectively. Because secondary phases and magmatic minerals have different Ca-Cl-K signatures and release Ar at different oven temperatures (Villa et al. 1996, 2000), the Cl/K and Ca/K ratios of every step give information on the mineral that underwent in-vacuo breakdown during each step. Common-denominator three-isotope correlation diagams have been validated by direct comparison with electron microprobe determinations of Ca/K and Cl/K ratios of heterochemical phases (Villa et al. 2000, their Fig. 4). By complementing the Ar data with CL and BSE images we can confirm the mineralogical heterogeneity and identify the Ca/K and/or Cl/K ratios of the unaltered phase, which we wish to date.

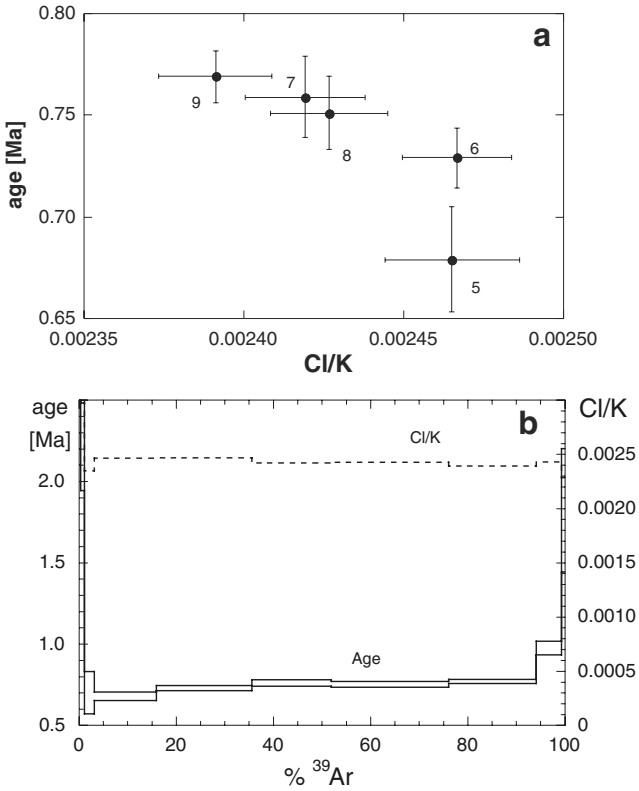


**Fig. 3** **a** Cl/K vs age plot ($^{38}Ar_{Cl}/^{39}Ar_K$ vs $^{40}Ar^*/^{39}Ar_K$) of phlogopite PG5 (Lower Ignimbrite, Fara d'Olivo Subsynthem). Steps 6 to 9 define an array with negative slope ($r^2$=0.99), indicative of a slight chemical heterogeneity. These steps correspond to an isochron with atmospheric intercept; the age of 753±15 ka is close to the more precise sanidine weighted average age of 739±12 ka. **b** Age spectrum (*solid lines*) and Cl/K spectrum (*dashed*). In Fig. 3a the linearity of the correlation trend can be immediately evaluated

## $^{39}Ar$-$^{40}Ar$ geochronology

A volcanic eruption frequently entrains lithic fragments of the basement. Such fragments can bias the age information, especially when performing bulk K-Ar analyses. The severity of the bias is increased in volcanic systems where magmas cross a thick, polygenic, old volcanic or old crystalline basement (Lo Bello et al. 1987). Monte Vulture lacks such an old basement. Coherently with this geological fact, it had been demonstrated by Villa (1988), by analysis of a 5-grain sanidine fraction, that bulk rock, pumice, and oligograin analyses gave exactly the same age spectrum, and that xenocrysts are not an issue affecting the sanidines of the basal Vulture samples. Xenocryst contamination may however be one of the many problems affecting biotite in the latest eruptions (see § 4.1.8).

In addition to the xenocryst problem, or the absence thereof at Vulture, in the volcanistratigraphic literature of the past decades there is a more profound misunderstanding about discrepant ages. It has been customary, in a part of the scientific community, to dismiss all ages that conflict

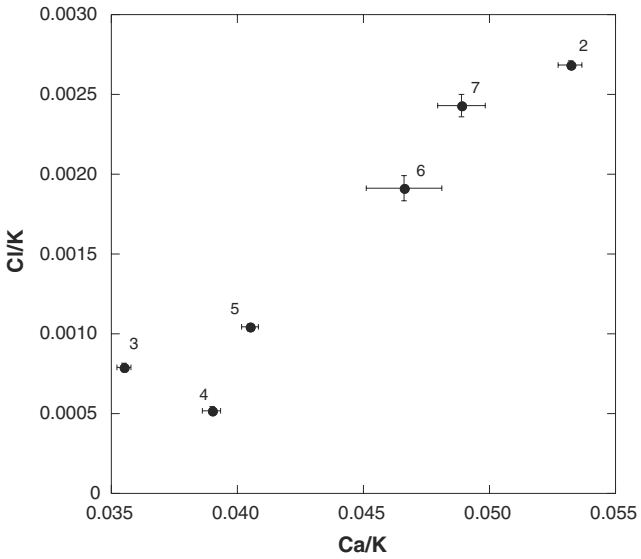


**Fig. 4** Chemical correlation diagram (Cl/K vs Ca/K) of sanidine VU 1680 from the Rionero Subsynthem. This sample has an extremely high Cl concentration of 710 ppm; only steps 3 to 5 show low Cl/K ratios. These three steps suggest an age ≤720±15 ka. Additional graphic representations are found as on-line supplementary material

with the rest of the stratigraphy with the blanket explanation of "excess Ar". In so doing, no attention is paid to the role of microtextures and high- or low-temperature alteration. In radical contrast to such a reductionist view, we clearly document with our photographs that deuteric high-temperature reaction microtextures are the most likely explanation for some discordant ages from Vulture. Moreover, deuterized minerals do not occur as discrete grains, but instead as ubiquitous μm-sized microstructures invisible to the naked eye and to the optical microscope. And precisely this point reveals that there is no factual difference between our mg-sized multi-grain fractions and laser-probe oligo-grain analyses (sometimes incorrectly referred to as single-grain analyses). If handpicking under the microscope, with visual resolution of about 50 μm, were sufficient to ensure ideal purity of oligo-grain fractions, then our handpicked fractions of a few mg would be just as clean: the only difference being that we chose to spend about 10–20 times more time handpicking fractions of 200–500 grains. Indeed, laserprobe analyses on a few grains have long been shown to be completely equivalent to furnace analyses on a few more grains (Wijbrans et al. 1990). The real discriminant is instead the need to characterize microtextures at sub-μm level. The realization that chemical disequilibrium textures are common and therefore influence the isotopic record has come of age in the recent geochronological literature on metamorphic rocks (e.g. Vance et al. 2003), but had never been extended to volcanic rocks so far. The presumed "rapid quenching" of volcanic minerals was not thought to be compatible with deuteric chemical disequilibrium textures that we document here for the first time. We propose that imaging should become routine in volcanic geochronology as well.

In order to cope with the presence of mineral mixtures stemming from the internal heterogeneity of the minerals, chemical correlation diagrams (Villa 2001) are a very powerful tool. A validation of that approach is provided by the observation that mineral breakdown during stepwise heating, laserprobe spot analyses, and chemical microanalyses by electron microprobe can all be tied together (Müller et al. 2002). We note that in order to investigate the Ca-Cl-K correlation diagrams it is of vital importance to measure the Cl/K ratios above the $^{38}$Ar detection limit. As this is not always possible with oligograin fractions of Cl-poor minerals, a paradoxical consequence is that laserprobe age determinations are potentially less accurate than those of mg-sized fractions if they do not allow a test of Ca-Cl-K systematics.

Thus, a mixture of heterochemical minerals can be unravelled if one has stoichiometric or microanalytical criteria that identify the target mineral by its Ca-Cl-K systematics and set it apart from its contaminants. Simple examples are the Ca/K ratio in mica separates and the Cl/K ratio in feldspars (both multigrain and oligograin analyses show exactly the same behaviour): stoichiometry requires both ratios to be zero in an ideal sample. Therefore, only the steps with the lowest values for these ratios should be considered as representing the unaltered, uncontaminated mineral reservoir. In the majority of our samples, the low Ca/K and/or Cl/K ratios are observed in several steps (not necessarily contiguous ones); we shall term these steps having constant and low Ca/K and Cl/K ratios "isochemical steps" as they represent the degassing of an isochemical reservoir.

Only isochemical steps were used for isochron and average age calculations and are marked by an asterisk in Table A2. All stratigraphically reliable ages are summarised in Table 1. As a general remark, it should be noted that the uncertainties of isochrons and averages are larger than those of individual steps. This is an effect of the scatter of the data points, itself an effect of the samples' mineralogical complexity. Furthermore, the phyllosilicates of Monte Vulture (biotites and phlogopites) are characterised by overall non-stoichiometric K contents, which is a likely monitor of significant deuterization. Moreover, sub-continental phlogopite retains a substantial amount of "parentless $^{40}$Ar" originating in the mantle (Wartho and Kelley 2003). Therefore, the chronological information provided by mantle-derived phlogopites is dubious. We present the Ar analyses of these mineral phases mainly for reasons of completeness. The chronological discussion will be hereafter based on the more reliable results provided by feldspar and leucite sepa-

rates. The discussion of mica data is omitted whenever feldspars or feldspathoids are available.

In the following we present re-evaluated and new data in stratigraphical order.

## New $^{39}$Ar-$^{40}$Ar analyses

### *Fara d'Olivo Subsynthem*

The Fara d'Olivo Subsynthem (Tables 1, A1) contains two large ignimbrite deposits, Lower and Upper Ignimbrite, which are separated by a paleosol. For the Lower Ignimbrite two sample analyses are available: an analysis of sample VU 1809 by Villa (1988, re-evaluated in § 4.2) and the new measurements on both sanidine and phlogopite of sample PG5 from a different outcrop. For the Upper Ignimbrite, in this study we analyzed sanidine separates VU 1813 A and VUT 9905; VU 1813 A is an aliquot of VU 1813 T of Villa (1988; see § 4.2).

For sanidine PG5 we have chemical information via the Cl/K and Ca/K ratios showing a remarkable inhomogeneity in the low temperature steps (probably due to imperfect manual separation). The weighted average of isochemical steps (that contain 52% of the total Ar) provides an age of 737±16 ka. The $^{39}$Ar-$^{40}$Ar analysis of the PG5 phlogopite offers the comparison with the coexisting sanidine. A Cl/K-age correlation diagram (Fig. 3) for gas-rich steps 6–9 shows only a weak dependence on chemical composition, which itself is fairly uniform, having Cl/K between 0.00239 and 0.00247. The average age of steps 6–9 is 753±15 ka. These same steps give an isochron with an atmospheric intercept of 289±12 and an age of 807±88 ka (MSWD=1.5), which is indistinguishable from the isochemical age.

Sanidine VUT 9905 from the stratigraphically younger Upper Ignimbrite of the Fara d'Olivo Subsynthem (Table 1) was separated from selected pumices. Its age spectrum shows internal discordance. Five gas-rich steps have an almost uniform chemical signature ($0.011<Ca/K<0.024$ and $0.000115<Cl/K<0.000156$; $^{39}$Ar=58% of total). The isochron through them gives an age of 735±58 ka with a trapped $^{40}$Ar/$^{36}$Ar ratio of 370±74. An isochron through six gas-rich steps of sanidine VU 1813 A gives 781±29 ka with an $^{40}$Ar/$^{36}$Ar initial ratio of 314±18. Unlike the Lower Ignimbrite, the Upper Ignimbrite samples appear to reproducibly have trapped a non-atmospheric Ar.

### *Spinoritola Subsynthem*

The Spinoritola Subsynthem consists of mafic dykes intruding the sedimentary basement. The samples we dated have no exposed stratigraphic relation to the other synthems. One dyke (sample VUT 110; Table A1) was analyzed three times: an acid-leached K-feldspar separate (Villa unpublished data 1988, re-evaluated here), and unleached separates in Bonadonna et al. (1998) and in the present work.

Our analysis of VUT 110 A was performed on a minute aliquot of the fraction analyzed by Bonadonna et al. (1998). From steps 2 to 8 with low Ca and Cl we calculated an isochron age of 698±48 ka and an initial $^{40}$Ar/$^{36}$Ar ratio of 339±31, marginally different from the atmospheric value. Therefore individual step ages (calculated with the assumption that $^{40}$Ar/$^{36}$Ar=295.5) are thought to be less reliable than the isochron age.

Villa (unpublished data 1988) had leached sanidine VU 110 with diluted HF (hereafter VU 110 L; Table A2) to get rid of visible alteration. However, no $^{37}$Ar and $^{38}$Ar data were acquired, disabling chemical correlations. We presume that the sanidine residuum after leaching was mostly alteration-free (as indicated by its much higher K concentration) and that its age represents that of the sanidine *sensu stricto*. The gas-rich steps from VUT 110 L provide an almost flat spectrum averaging 678±9 ka, indistingushable from the isochemical age of untreated aliquot VUT 110A. The identity of the isochemical age, which required post-analytical removal of heterochemical steps on the basis of Ca/Cl/K ratios, with the leach residue age, which is thought to result from physical removal of heterochemical phases, is evidence that our interpretive approach is legitimate.

Sanidine VUG 1 derives from another dyke of the Spinoritola Subsynthem (Table A1). This sanidine is low in $K_2O$ with a variable but high Cl content (288 ppm; Table A2). Again, the age spectrum shows internal discordance. As the presence of Cl is indicative of non-feldspathic phases, we chose the chemically most homogeneous, low Cl-steps, which yield a weighted average of 698±25 ka for this sample.

### *Toppo San Paolo Subsynthem*

A sanidine separate from the Toppo San Paolo lava dome (VUG 61) was analysed. Steps 5 to 13, containing 77% of the total gas, have a uniform chemical signature: Ca/K= 0.026 to 0.036, Cl/K=0.0010 to 0.0036. An average age of all these steps gives 673±19 ka. An average of the last three steps, having Cl/K<0.0016, gives 671±37 ka, identical to the previous one, but less precise. This indicates that minor variations in the Cl/K ratio in this particular sample do not reflect secondary alterations but are a primary feature; this only applies to Cl/K ratios<0.0036, as steps with higher Cl/K ratios do deviate from the above average age.

### *Rionero Subsynthem*

Two sanidine separates (VU 1680 and VUT 0002) of a fallout deposit from the Masseria Boccaglie plinian erup-

tion have been analyzed. Sanidine VU 1680 A was an aliquot of the sample VU 1680 used by Villa (1988) and Brocchini et al. (1994). Coexisting leucite is analcimized (Villa 1988) and was not re-analyzed. The age spectrum of the sanidine is discordant. Most of the Ar was released between 550 and 820°C, i.e. at much lower temperatures than all other sanidines (Table A2) reproducing the pattern obtained by Villa (1988). This observation, in combination with the petrographical observation of a patchy appearance visible in the CL-image (Fig. 2c), indicates that the structure of the VU 1680 sanidine was heavily damaged during high-temperature alteration. Indeed, this sanidine is characterised by a very high Cl concentration (710 ppm), indicating that it should not be considered as pristine. Basing on the Cl/K and Ca/K ratios (Table A2), a group of data points with lowest amounts of Cl and Ca (steps 3 to 5) can be discriminated from steps having up to two orders of magnitude higher Cl/K ratios. The isochron through the three low Cl-steps results in no age as the regression line is horizontal; their step ages suggest an age $\leq 720\pm15$ ka.

Sanidine VUT 0002 (Table A1) derives from a different outcrop of the same pumice fall deposit as the previous sample. It contains substantially less Cl than VU 1680 and provides an isochemical low Ca/K, low Cl/K group of steps 2 to 5 (containing 63 % of the total gas) with an average of 714±18 ka. This estimate is indistinguishable from our analysis of VU 1680, but is more reliable owing to the less pervasive alteration.

*Vulture San Michele Subsynthem*

We analysed a total of four samples of this subsynthem, phlogopite/biotite samples VUT 9918, VUT 9919 and VUT 9923 and leucite VU 1907 A. In the following we focus only on one phlogopite (VUT 9918) as a representative for all mica analyses and on the leucite VU 1907 A.

Sample VUT 9918 derives from a small lava flow that represents the final eruptive event of a small scoria cone. This cone is situated at the top of the stratigraphic sequence of the Vulture San Michele Subsynthem. A phlogopite separate reveals a grossly sub-stoichiometric K concentration and accordingly a staircase-shaped $^{39}$Ar-$^{40}$Ar spectrum. It is important to understand the petrological implications of such a pattern. Staircase-shaped age spectra are not indicative of a concentric Ar zonation such as could result from diffusive Ar loss, as the combined laser-oven analysis of zoned biotite grains gave a flat age spectrum (Hodges et al. 1994). Instead, staircases have been documented both in the case of alteration (Hess et al. 1987) and in the case of unaltered mixed generations (Villa et al. 1997). Focussing on gas rich steps, 4 to 7, a good anticorrelation ($r^2$=0.80) between Cl/K-ratio and corresponding ages is visible (Fig. 5). This implies that $^{39}$Ar recoil into chlorite has no influence on this sample (cf. Fig. 7). The anticorrelation in Fig. 5 indicates the presence of two phases having different Cl contents and different apparent ages. An isochron calculation would thus combine non-cogenetic systems and should therefore not be considered. The lowest step age is 691±25 ka. A mantle origin is very likely for these large phlogopite xenocrysts (Stoppa and Principe 1997; Jones et al. 2000; Downes et al. 2002). It is not surprising that phlogopite should incorporate mantle Ar with $^{40}$Ar/$^{36}$Ar >> 300 and so give an unreliable age.

Leucite of sample VU 1907 derives from one of the stratigraphically youngest lava flows of the Vulture San Michele Subsynthem. An aliquot, labelled as VU 1907 A, of the leucite analysed by Brocchini (1993) was analysed in this study. It reveals a nearly stoichiometric $K_2O$ content of 20 wt% and a total Cl concentration of 69 ppm and shows a discordant, hump-shaped age spectrum (Fig. 6). The degassing occurs at low temperature, as expected from leucite. The Ca/K and Cl/K ratios are linearly correlated, indicative of a binary mixing. The phase with low Ca/K and low Cl/K ratios has the typical chemical signature of our leucite electron microprobe analyses. We will consider steps 5 and 6 with the lowest Cl/K ratio and an average age of 609±9 ka (Table A2) to most closely approximate the leucite *sensu stricto*. Our images on few leftover grains (Fig. 2a, b) show no inhomogeneous K distribution and no alteration.

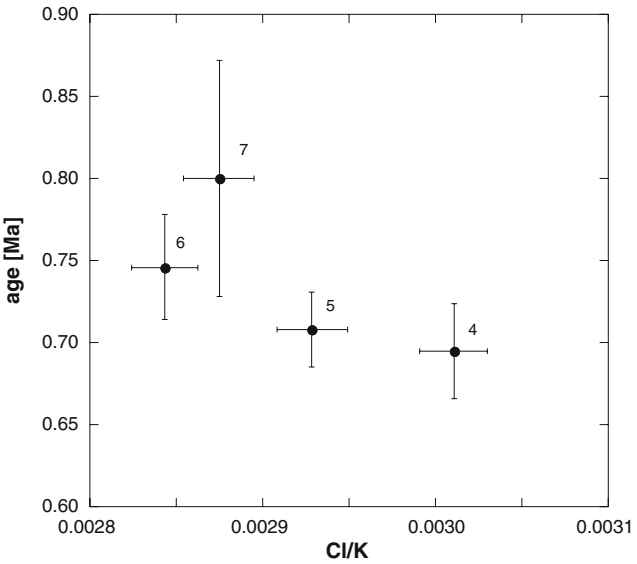


**Fig. 5** Cl/K vs age diagram of phlogopite VUT 9918 (Vulture San Michele Subsynthem) with an anticorrelation ($r^2$=0.80) between ages and Cl/K ratios. The age information provided by the lowest step age is still affected by excess Ar of possible mantle origin. Additional graphic representations are found as on-line supplementary material

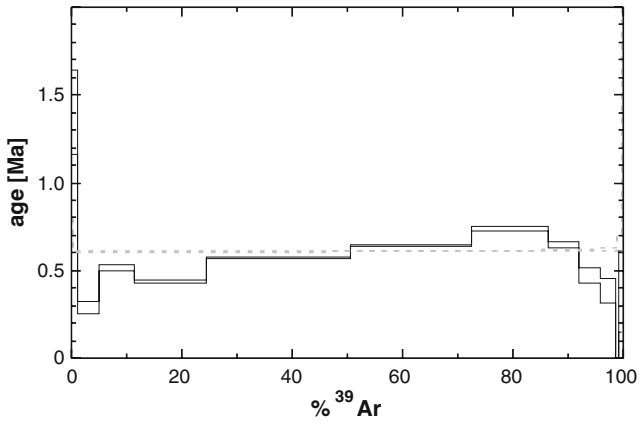


**Fig. 6** Age spectra of leucite VU 1907 (*grey dashed line*: Brocchini 1993; *solid black line*: this study). The average age of the two data-sets is 610±8 ka. Additional graphic representations are found as on-line supplementary material

*Case Lopes Subsynthem*

After a period of volcanic quiescence that lasted for several tens of ka (as suggested by the deposition of a 1.5 m thick paleosol, M18: Brocchini et al. 1994), volcanism resumed as a result of an intensive volcano-tectonic activity (Brocchini et al. 1994). Sample VUT 168 from the Case Lopes Subsynthem was collected in a scoriae deposit related to the normal fault system of Valle dei Greggi-Fosso del Corbo. Biotite yields a discordant age spectrum (Fig. 7a).

A widespread feature of sheet-silicates, such as biotite, is the intergrowth of chlorite, a phase affecting $^{39}$Ar-$^{40}$Ar systematics. Biotite VUT 168 is a likely candidate of such an intergrowth, as its K concentration is significantly sub-stoichiometric. In a three-isotope correlation plot (Fig. 7b) the trajectory of data-points defines two different temperature-dependent trends. Path A between step 2 and step 4 (corresponding to furnace temperatures between 624 and 771°C) results in a negative slope. This pattern is likely to result from degassing of heterochemical impurities. The trajectory between steps 4 and 5 has a positive slope, i.e. a correlated increase of the $^{40}Ar^*/^{39}Ar_K$ ratio and the $^{38}Ar_{Cl}/^{39}Ar_K$ ratio. This may reflect ca. 20% recoil loss of $^{39}Ar_K$ during irradiation, as indicated by the dashed line in the inset of Fig. 7b. Such a $^{39}Ar_K$ recoil loss may be associated to the presence of fine (≤ 0.1 μm) chlorite lamellae (see, e.g., Di Vincenzo et al. 2003). Finally, path B (Fig. 7b), corresponding to decreasing Ar release, probably reflects the degassing of impurities with variable Cl/K and Ca/K ratios.

The chloritisation reaction and the attending, uncontrolled loss of $^{40}Ar^*$ as well as of K, combined with $^{39}Ar_K$ recoil, all hamper an age estimation. The total fusion age of 879 ka is meaningless. The weighted average of steps 4 and 5 that lie on the "chlorite-biotite line" (the line with a positive slope reflecting 1:1 variations in the denominator of the $^{38}Ar_{Cl}/^{39}Ar_K$ vs $^{40}Ar^*/^{39}Ar_K$ diagram; Fig. 7b, inset) suggests a maximum estimate of 530±22 ka. However, it must be emphasized that this estimate has a much lower reliability than all other isochron and isochemical ages of the present work.

*Lago Piccolo Subsynthem*

The mm-sized biotite crystals of sample VUT 251 derive from the most external shell of the tuffisitic lapilli that represent the juvenile fraction of the Lago Piccolo deposit. This biotite sample has a similar origin as the mica in tuffisitic lapilli sample VUT 0008 (see next paragraph) and shares common Ar-geochemical characteristics with it. All measured $^{40}Ar/^{36}Ar$ ratios are very close to atmospheric composition. The total $^{36}Ar$ concentration (a measure of the trapped Ar) is one order of magnitude higher in the

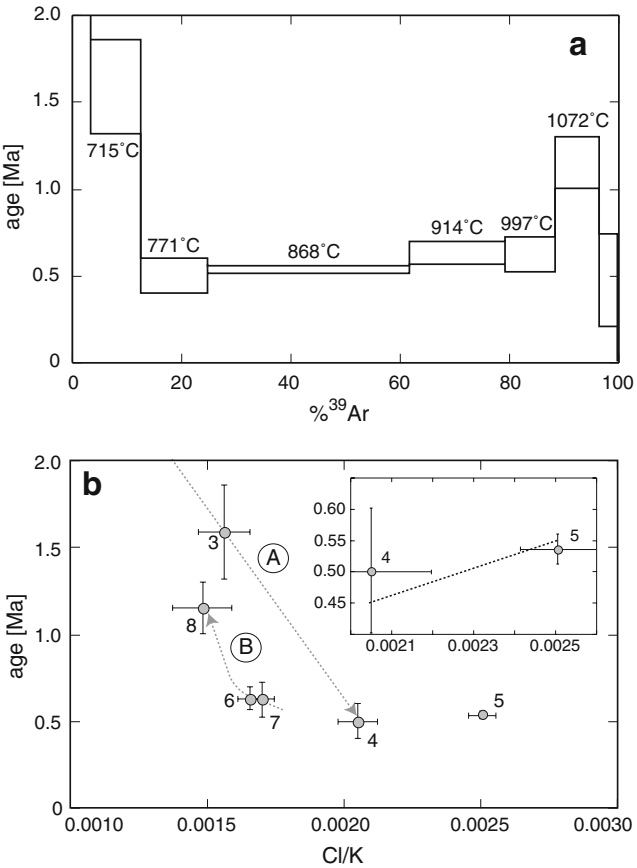


**Fig. 7** Age spectrum of biotite VUT 168 (Case Lopes Subsynthem). Some data points, labelled with corresponding step numbers, exhibit a negative correlation trend, denoted as A. It describes the alteration phases degassed below 770°C. The dashed line shown in the inset is the predicted effect of recoil in sub-μm biotite/chlorite intergrowths. A 20% recoil of $^{39}Ar$ out of biotite and its re-implantation in chlorite produces a 20% increase both in the x-values and in the y-values, which simulates a positive correlation. Steps 4 (771°C) and 5 (868°C), the most gas-rich one, probably reflect degassing of such a biotite-chlorite intergrowth. High temperature steps 6 to 8 (path B) reflect degassing of phases with higher and/or discordant Ca/K and/or Cl/K ratios. Additional graphic representations are found as on-line supplementary material

diatreme micas compared to a typical magmatic phlogopite such as PG5. The fraction analyzed here, labelled VUT 251 AB, is a vial aliquot of that analyzed by Brocchini (1993). The K concentration of biotite VUT 251 AB is not stoichiometric (6.7%), indicating a substantial high- or low-temperature alteration. The chemical indicators, Ca/K and Cl/K, identify the degassing of isochemical phlogopite *sensu stricto*, corresponding to Ca/K<0.05 and 0.0021<Cl/K<0.0024, at oven temperatures between 900 and 1,040°C. Isochron regression of the 900–1,040°C steps gives 121±15 ka. The calculated initial $^{40}Ar/^{36}Ar$ ratio is indistinguishable from, but about 1 % higher than, the atmospheric value. Step ages are therefore meaningless, because they are calculated on the incorrect assumption that $(^{40}Ar/^{36}Ar)_{trapped}=295.5$.

*Serra di Braida Subsynthem*

Sample VUT 0008 are tuffisitic lapilli from deposits of a diatremic eruption (Principe and Giannandrea 2002) near the Ripacandida village, east of Monte Vulture edifice. For reasons of comparison three different black-mica fractions were separated: one dark green phlogopite and two dark brown Mg-biotite fractions. The finer grained biotite fraction was obtained by grinding coarse (cm-sized) biotite in the mortar to eliminate visibly altered rims. Firstly, K concentrations range between 3.9 wt % for the large biotite and 5.1 wt % for the phlogopite (Table A2), demonstrating very heavy alteration. Grinding and hand-picking improved the K and Cl concentration, but only to a limited degree. Calculated isochron ages are 0.9±1.3, 0±2, and 1.1±0.8 Ma for the phlogopite, large biotite and small biotite, respectively. The extreme error enlargement with respect to individual steps is due both to the high MSWD (i.e. to excess scatter) and to the long and unfavourable extrapolation of the very unradiogenic data points. A diatreme eruption could contain both a juvenile magmatic mica and a reworked xenocrystic mica of undetermined origin: entrained from the pre-existing volcanic edifice, or from basement below the volcano, and/or mantle xenoliths (Downes et al. 2002; Jones et al. 2000). The near-atmospheric $^{40}Ar/^{36}Ar$ ratio measured in all steps makes the calculated age extremely sensitive to small admixtures of mantle Ar, to minor xenocrystic contamination (both giving a non-atmospheric trapped Ar), and to high- or low-temperature alteration during diatreme emplacement. The high MSWD of the isochron calculation is evidence that there was more than one trapped Ar composition, suggesting that all three effects may have played variable roles. As a result the calculated age is unreliable. As in the VUG 251 analysis, blank-corrected $^{36}Ar$ concentrations are one order of magnitude higher than in other Vulture phlogopites and two orders of magnitude higher than in Vulture feldspars. In this sample, the geochemistry of trapped Ar is prevalent over the geochronological usefulness.

## Context and discussion

In the following paragraph we compare our new analyses with published data and discuss the reliability of age estimates. In four cases we analysed the same samples as previous literature. In so far as these repeat analyses are truly duplicates performed on aliquots of the same sample material, it is legitimate to pool them into a grand average. Note that, from a statistical point of view, a pooled isochron is more justified than a pooled plateau average. In the latter case, the isotopic composition of the trapped Ar is always assumed to be equal to atmospheric Ar. In the former, the trapped Ar is a priori unknown, and is obtained by least squares fitting. Even if (in both cases) a coincidence within analytical uncertainty is expected, it is still possible that in two isochrons on repeat aliquots the calculated trapped Ar of one be significantly different from atmospheric Ar, while that of the other one be indistinguishable from it. If so, averaging the inaccurate plateau of the former with the plateau of the latter would be illegitimate.

Among the four duplicate analyses that we performed, samples VU 1907 and VUT 251 are dry aliquots of the same sample bottle analysed in the past, and pooling is straightforward. The matter is slightly more complicated for the sample pair from the Lower Ignimbrite, VU 1809 / PG 5. Because both samples actually represent the same magma, sampled in different localities but certainly pertaining to the same eruption, we feel justified in pooling the isochrons (see below), obtaining a smaller uncertainty on an otherwise unchanged central age. The least constrained case is that of the Upper Ignimbrite sample pair, VU 1813 / VUT 9905 (see below), for which non-atmospheric intercepts are obtained. In this case, no precise age assignment can be reliably inferred from the $^{39}Ar$-$^{40}Ar$ data, pooled or unpooled.

From the Fara d'Olivo Subsynthem, an analysis of sanidine VU 1809 from the Lower Ignimbrite was reported by Villa (1988), without the information on $^{37}Ar$ and $^{38}Ar$. The age spectrum has a slight saddle shape; the weighted average age of 6 steps released at intermediate furnace temperatures and containing 72% of the total Ar is 742±22 ka. This age is indistinguishable from our new results of sample PG 5. A pooled isochron of gas-rich steps of both sanidines VU 1809 and PG 5 from the Lower Ignimbrite of the Fara d'Olivo Subsynthem is justified by their identical magma source. After scaling for different irradiation intensities, it gives an age of 732±23 ka with an atmospheric intercept of 297±3 and an MSWD of 1.7. Therefore, it is justified to use the pooled weighted average of the steps between 850 and 1,300°C from both samples and we consider 739±12 ka as the best estimate of the age of the Lower Ignimbrite.

In a literature comparison of the two large ignimbrites of the Fara d'Olivo Subsynthem, the stratigraphically younger Upper Ignimbrite gives slightly older apparent ages than the Lower Ignimbrite. Villa (1988) reported three analyses of sample VU 1813 from the Upper Ignimbrite: VU 1813 P (handpicked single sanidine grains from a pumice), VU 1813 T (sanidine from the unseparated whole rock) and VU 1813 L leached with diluted HF. According to Villa (1988) the three fractions of sanidine VU 1813 (P, T, L) are characterised by the presence of excess $^{40}Ar$ ($^{40}Ar_{xs}$) and show similar saddle-shaped spectra. A regression through the original data gives no statistically acceptable isochron; as at that time the $^{37}Ar$ and $^{38}Ar$ were not acquired, it is impossible to evaluate the chemical identity of reservoirs and thus to calculate an average of isochemical steps. Nevertheless, the isochron diagram clearly shows trapped Ar with an enriched $^{40}Ar/^{36}Ar$ ratio and confirms the presence of $^{40}Ar_{xs}$. It is further possible to plot all analyses of the Upper Ignimbrite in one isochron diagram. Most fits through reasonable subsets of the data always produce ages not far from the age of the Lower Ignimbrite, 739±12 ka.

From the Spinoritola Subsynthem, two additional analyses of samples VUT 110 and VUG 1 had been performed previously. Bonadonna et al. (1998) present an isochron age of 674±7 ka for sample VUT 110 (Table 1). The original data (Brocchini 1993) show a clear chemical heterogeneity with Ca/K ratios between 0.045 and 0.37 and Cl/K ratios between 0.0014 and 0.0126. This heterogeneity discourages regression of different, possibly non-cogenetic phases. We recalculated an isochron of isochemical steps only, and obtained an age of 698±16 ka, using the updated FC age. We note that the chemical composition of VUT 110 A (K=7.3%, Cl=96 ppm, Ca=0.2%) is unlike that of the Bonadonna et al. (1998) analysis (K=9%, Cl=202 ppm, Ca=0.5%). The heterogeneity of two aliquots from the same sample container is a likely electrostatic effect of almost empty plastic vials.

The four analyses of samples VUT 110 and VUG 1 all give ages below 700 ka (Table 1). Thus, the definition of the Spinoritola Subsynthem as the earliest volcanic manifestation (Principe and Giannandrea 2002) requires a re-examination, as its age is significantly and reliably younger than that of the Fara d'Olivo Subsynthem ignimbrites.

From the Rionero Subsynthem, two $^{39}Ar$-$^{40}Ar$ analyses, VUT 140 and VUT 146, were published by Bonadonna et al. (1998). Our recalculation based on isochemical steps and the revised FC age gives ages of 672±6 ka and 630±20 ka (Table 1), respectively. The Rionero Subsynthem is complex and has a considerable thickness, and it is to be expected that it was deposited over a fairly long timespan. The age difference between the lowest sample (VUT 0002) and one of the highest ones (VUT 146) is 84±28 ka. Also note that this subsynthem overlaps temporally with the emplacement of the monogenic Toppo San Paolo lava dome at 673±19 ka.

From the Vulture San Michele Subsynthem, the abstract by Villa (1985) reported an analysis on what was labelled as "leucite VU 1907" (without providing chemical information); however, the degassing behaviour above 600°C was very untypical of leucite. As the unusual degassing pattern was never reproduced by the subsequent analyses of leucite VU 1907, it is possible that a sample mislabelling could have occurred. Because of that possibility, and the absence of analytical data, that report should not be given undue importance. According to our recalculation of the data given by Brocchini (1993), the average age of their low Cl/K and low Ca/K steps provides an age of 611±12 ka. The pooled isochron regression through the low-Ca, low-Cl steps from our analyses and those of Brocchini (1993) shows no significant non-atmospheric intercept. The isochron age of 590±12 ka corresponds to a high MSWD of 18, but because of the atmospheric intercept it is indistinguishable from the average of isochemical step ages. Therefore, we propose that the grand average of low-Ca, low-Cl step ages, 610±8 ka, accurately dates the eruption.

The fallout deposits of the Ventaruolo Subsynthem (NW of Rionero and W of Melfi) are ascribed to the uppermost sequence of the Barile Synthem. We re-evaluated the phlogopite age of sample VUT 256 on the basis of the data in Brocchini (1993), using the revised FC age and by only taking into account isochemical steps 2 to 6. The resulting weighted average age of 671±17 ka, however, has to be considered as a maximum estimate as the phlogopite is characterised by an excess Ar component (initial $^{40}Ar/^{36}Ar$ ratios from isochron calculations performed on

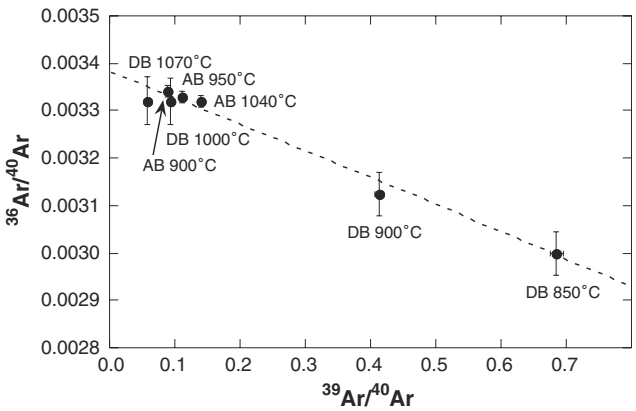


**Fig. 8** Isochron of sample VUT 251 from the Lago Piccolo Subsynthem. Three points labelled AB are the isochemical steps from the present work; oven temperatures are also indicated. Four points labeled DB are the isochemical steps selected from Brocchini (1993); oven temperatures are seen to be coincident. The calculation of an isochron provides an age of 146±9 ka with an atmospheric $^{40}Ar/^{36}Ar$ intercept of 295±1

different subsets are always >330). Rather than the phlogopite data, it is the stratigraphic relation to the underlying subsynthems, Rionero (latest dated eruption at 630±20 ka) and Vulture San Michele (latest dated eruption at 610±8 ka), that provide a more stringent constraint on the age of the Ventaruolo Subsynthem.

The Castello di Melfi Subsynthem consists of a small lava flow with a peculiar mineral assemblage (Melfi haüynophyre, Hieke Merlin 1967), which was extruded along a NW-SE trending fault subsequent to the build-up phase of the stratovolcano. The original leucite sample (VU 1523) analysed by Villa (1991), Brocchini et al. (1994) and Bonadonna et al. (1998) is no longer available. Our attempt to date the coexisting noseane failed; the step ages are grossly discordant and range between −8.3 and +26.5 Ma, in no apparent correlation with the Ca-Cl-K indicators. The deuteric microstructures imaged in Fig. 2e may be responsible both for the disturbance of the K-Ar clock and for a variable recoil-derived redistribution of $^{37}$Ar, $^{38}$Ar and $^{39}$Ar. According to Villa (1991), leucite VU 1523 has an age of 565±4 ka relative to the B4M irradiation monitor at 18.6 Ma (Flisch 1982). From data presented in Bonadonna et al. (1998), a recalculated age of 573±4 ka is obtained using the revised FC age and averaging only the gas rich isochemical steps.

From the Case Lopes Subsynthem, the data of VUT 168 given by Brocchini (1993) were recalculated using the revised FC age and restricting the average to the Cl-poor, gas-rich steps. The revised age, 494±5 ka, is similar to our own given in § 4.1.6, 530±22 ka. This similarity demonstrates the reproducibility of analyses, but *per se* gives no information on accuracy. On the contrary, it needs to be repeated that on account of the non-stoichiometry this mica age should be viewed with extreme caution. Therefore we do not assign an age to this subsynthem in our Table 1.

As for the Lago Piccolo Subsynthem, independent age constraints on the formation of the lakes are very scant. Lake formation post-dates the collapse of the volcanic edifice (certainly <610±8 ka, probably younger than ca. 500 ka, depending on the uncertain age of the Case Lopes Subsynthem) and pre-date counted varve deposition in the lake sediments (ca. 100 ka: Wulf et al. 2004). Brocchini (1993) presents data for a powder aliquot of sample VUT 251 from the Lago Piccolo Subsynthem (hereafter coded as

**Table 1** Chronostratigraphy of Monte Vulture volcano

| Ssy | Synthem | Subsynthem | Sample | Age/ka | Recommended age/ka |
|---|---|---|---|---|---|
| **Monticchio** | **Laghi di Monticchio** | Lago Piccolo | VUT 251 | **141±11**<br>**160±17$^{(B)}$** | **141±11** |
| | **Valle dei Greggi-Fosso del Corbo** | Case Lopes | VUT 168 | **530±22**<br>**494±5$^{(B)}$** | |
| **Monte Vulture** | **Melfi** | Castello di Melfi | VUT 1523 | **573±4$^{(B)}$**<br>**565±4$^{(D)}$** | **573±4$^{(B)}$** |
| | **Barile** | Ventaruolo | VUT 256 | **<671±17$^{(B)}$** | **<610** |
| | | Vulture-San Michele | VUT 1907 | **609±9**<br>**611±6$^{(B)}$** | **610±8** |
| | | Rionero | VUT 140<br>VUT 146 | **630±20$^{(A)}$**<br>**672±6$^{(A)}$** | **From 630±20 to 714±18** |
| | | | VUT 0002 | **714±18** | |
| | | | VUT 1680 | **<720±15** | |
| | | Toppo San Paolo | VUG 61 | **673±19** | **673±19** |
| | **Foggianello** | Spinoritola | VUG 1<br>VUT 110 A | **698±25**<br>**698±48** | **687±8** |
| | | | VUT 110 L | **678±9** | |
| | | | VUT 110 | **698±8$^{(A)}$** | |
| | | Fara d'Olivo | VUT 9905<br>VU 1813 | **<755±21**<br>**<781±29** | **U.I: <739** |
| | | | VU 1809<br>PG 5 (phl.) | **742±22$^{(C)}$**<br>**753±15** | **L.I: 739±12** |
| | | | PG 5 (san.) | **737±16** | |

Synthems follow Giannandrea et al. 2002; not all subsynthems are shown, but only those for which an $^{39}$Ar-$^{40}$Ar analysis was obtained. Each accepted age refers to one single sample (indicating the weighted average or the most reliable assignment where duplicate analyses were performed). Multiple ages for some subsynthems refer to stratigraphically distinct units. Recalculated ages from (A) Bonadonna et al. (1998); (B) Brocchini 1993; (C) Villa (1988); (D) Villa (1991); no superscripts = this work. Ssy = Supersynthem; L.I. = Lower Ignimbrite; U.I. = Upper Ignimbrite

VUT 251 DB). Our re-analysis of the original data (Brocchini 1993) in context with our own data allows a reliability assessment. The K concentration of VUT 251 DB can be calculated as 7.8 %, indicating that the "empty plastic vial" electrostatic artefact left behind a residue (our fraction VUT 251 AB) more enriched in alteration phases. All measured $^{40}Ar/^{36}Ar$ ratios are <330, that is, less radiogenic than most other samples. This confirms the predominant role of trapped Ar relative to radiogenic Ar, and consequently the sensitivity of calculated ages on the assumed isotopic composition of trapped Ar. The Ca/K vs. Cl/K discrimination identifies the four steps between 850 and 1,070°C as the "true" phlogopite (Ca/K<0.02, 0.0025< Cl/K<0.0032). Both the release temperatures and the chemical fingerprint (considering the possible intercalibration uncertainties in reactor production rates of $^{38}Ar$ from Cl) are identical in fractions AB and DB, and support the identity of the principal gas carrier in the two analyzed separates. Therefore, it is justified to perform a joint regression of both analyses; this is shown in Fig. 8. The isochron age is 146±9 ka. The trapped Ar is calculated as $^{40}Ar/^{36}Ar=295\pm1$. The atmospheric intercept shows that step ages are accurate; the weighted average of the seven combined isochemical steps that pertain to "true" phlogopite of VUT 251 AB and DB gives 141±11 ka. This age is the most reliable estimate of the Monticchio phlogopites.

## Conclusions

Our $^{39}Ar$-$^{40}Ar$ investigations on different minerals of Monte Vulture volcanics from several eruptive phases confirm and refine previous geochronological work. Reproducible, internally discordant age spectra, and the attendant increased uncertainties of age assignments, are the result of intra-grain heterogeneities of the analyzed minerals. Deep deuteric processes, typical of many Vulture rocks, led to transformation of mineral phases; therefore, the loss of LIL elements such as K (and its decay product Ar) is likely to occur. Mineralogical and microchemical investigations demonstrate deuterization effects (moderate to strong) in sanidine and phlogopite; leucite is analcimized in many rocks, but leucite samples of the present work have uniform and almost stoichiometric microchemical K distributions. Since our phlogopite samples have always substoichiometric K concentrations, an appropriate interpretation of Ar systematics needs to consider the effects of chloritisation combined with $^{39}Ar_K$ recoil during neutron irradiation. Many analyzed phlogopites give dubious or inaccurate ages. Instead, we focussed our chronostratigraphic conclusions on leucite and sanidine. As in all tectosilicates, secondary reactions are revealed by elevated Cl/K ratios. The combination of Ca-Cl-K systematics with microtextural and microchemical analyses is the only means to see through deuteric processes.

By taking into account chemical heterogeneities of primary and secondary origin, it is possible to derive highly reliable age estimates. These constrain the main volcanic activity to a narrow time interval between ca. 740 ka and 610 ka (Table 1). During this time span the composite stratovolcano was built up.

Subsequently to the main volcanic activity, the small, isolated Melfi haüynophyre was extruded at 573±4 ka. Other, mainly monogenetic centers, aligned along the main active tectonic trends, became active in the Vulture area around this time. After a very long quiescence time gap, final stages of volcanism are characterised by formation of maars; the very prominent Lago Piccolo di Monticchio deposit was dated at 141±11 ka.

**Acknowledgements** This work was partly supported by Swiss National Science Foundation grants No. 21-63866.00 and 200020-100230. I.M.V. wishes to warmly thank Luigi La Volpe for many discussions and for starting the dating work a long time ago together with Sergio Borsi and Giorgio Ferrara, who both did not live to see it completed. Over two decades, Carlo Quercioli and Giuliana De Grandis separated mineral phases from samples of Monte Vulture collection at Istituto di Geocronologia, Pisa. Claudia Principe provided VUT and PG samples. Edwin Gnos and Karl Ramseyer greatly helped to characterize mineral microtextures. Three anonymous referees and Associate Editor Raffaello Cioni provided constructive criticism.

## References

Bonadonna FP, Brocchini D, Laurenzi MA, Principe C, Ferrara G (1998) Stratigraphical and chronological correlations between Monte Vulture volcanics and sedimentary deposits of the Venosa basin. Quatern Int 47(48):87–96

Brocchini D (1993) Il Vulcano Vulture (Basilicata). Cronologia radiometrica ed evoluzione. Unpublished MSc thesis, Univ Pisa: 1–70

Brocchini D, La Volpe L, Laurenzi MA, Principe C (1994) Storia evolutiva del Mt. Vulture. Plinius 12:22–25

Cortini M (1975) Età K-Ar del Monte Vulture (Lucania). Rivista Ital Geofis Scienze Affini 2:45–46

De Astis G, Kempton PD, Peccerillo A, Wu TW (2006) Trace element and isotopic variations from Mt. Vulture to Campanian volcanoes: constraints for slab detachment and mantle inflow beneath southern Italy. Contrib Mineral Petrol 151:331–351

De Fino M, La Volpe L, Peccerillo A, Piccarreta G, Poli G (1986) Petrogenesis of Monte Vulture volcano (Italy): inferences from mineral chemistry, major and trace element data. Contrib Mineral Petrol 92:135–145

Di Muro A, Bonaccorsi E, Principe C (2004) Complex colour and chemical zoning of sodalite-group phases in a haüynophyre lava from Mt. Vulture, Italy. Mineral Mag 68:591–614

Di Vincenzo G, Viti C, Rocchi S (2003) The effect of chlorite interlayering on $^{40}Ar$-$^{39}Ar$ biotite dating: a $^{40}Ar$-$^{39}Ar$ laser-probe

and TEM investigations of variably chloritised biotites. Contrib Mineral Petrol 145:643–658

Downes H, Kostula T, Jones AP, Beard AD, Thirlwall MF, Bodinier JL (2002) Geochemistry and Sr-Nd isotopic compositions of mantle xenoliths from the Monte Vulture carbonatite-melilitite volcano, central southern Italy. Contrib Mineral Petrol 144:78–92

Flisch M (1982) Potassium-argon analysis. In: Odin GS (ed) Numerical dating in stratigraphy. Wiley, Chichester, pp 151–158

Giannandrea P, La Volpe L, Principe C, Schiattarella M (2002) Carta Geologica del Monte Vulture. 81 riunione estiva Soc Geol It Torino, 10–12 Sept 2002, abstract

Hess JC, Lippolt HJ, Wirth R (1987) Interpretation of $^{40}Ar/^{39}Ar$ spectra of biotites—evidence from hydrothermal degassing experiments and TEM studies. Chem Geol 66:137–149

Hieke Merlin O (1967) I prodotti vulcanici del Monte Vulture (Lucania). Mem Istituto Geol Mineral Univ Padova 26:1–67

Hodges KV, Hames WE, Bowring SA (1994) $^{40}Ar/^{39}Ar$ age gradients in micas from a high-temperature low-pressure metamorphic terrain —evidence for very slow cooling and implications for the interpretation of age spectra. Geology 22:55–58

Jones AP, Kostoula T, Stoppa F, Wooley AR (2000) Petrography and mineral chemistry of mantle xenoliths in a carbonate-rich melilititic tuff from Mt. Vulture volcano, southern Italy. Mineral Mag 64:593–613

La Volpe L, Principe C (1991) Comments on "Monte Vulture Volcano (Basilicata, Italy): an analysis of morphology and volcaniclastic facies" by JE Guest, AM Duncan, DK Chester. Bull Volcanol 53:222–227

Lo Bello P, Féraud G, Hall CM, York D, Lavina P, Bernat M (1987) $^{40}Ar/^{39}Ar$ step-heating and laser fusion dating of a quaternary pumice from Neschers, Massif Central, France: the defeat of xenocrystic contamination. Chem Geol 66:61–71

Melluso L, Morra V, Di Girolamo P (1996) The Mt. Vulture volcanic complex (Italy): evidence for distinct parental magmas and for residual melts with melilite. Mineral Petrol 56:225–250

Müller W, Kelley SP, Villa IM (2002) Dating fault-generated pseudotachylytes: comparison of $^{40}Ar/^{39}Ar$ stepwise-heating, laser-ablation and Rb/Sr microsampling analyses. Contrib Mineral Petrol 144:57–77

Peccerillo A (2005) Plio-Quaternary volcanism in Italy, Petrology, geochemistry, geodynamics. Springer, Heidelberg, p 365

Principe C, Giannandrea P (2002) Stratigrafia ed evoluzione geologica del vulcano Vulture (Basilicata, Italia)—Rapporti fra vulcanismo ed ambienti sedimentari. 81 riunione estiva Soc Geol It Torino, 10–12 Sept 2002, abstract

Ramseyer K, Fischer J, Matter A, Eberhardt P, Geiss J (1989) A cathodoluminescence microscope for low intensity luminescence. J Sedimentary Petrol 59:619–622

Renne PR, Swisher CC, Deino AL, Karner DB, Owens TL, DePaolo DJ (1998) Intercalibration of standards, absolute ages and uncertainties in $^{40}Ar/^{39}Ar$ dating. Chem Geol 145:117–152

Stoppa F, Principe C (1997) Eruption style and petrology of a new carbonatitic suite from the Mt. Vulture (Southern Italy): the Monticchio Lakes formation. J Volcanol Geothermal Res 78:251–265

Vance D, Müller W, Villa IM (2003) Geochronology: linking the isotopic record with petrology and textures—an introduction. In: Vance D, Müller W, Villa IM (eds) Geochronology: Linking the isotopic record with petrology and textures. Geol Soc London Spec Publ 220: 1–24

Villa IM (1985) Cronologia $^{39}Ar/^{40}Ar$ del complesso vulcanico del Monte Vulture. Rend Soc Ital Miner Petrol 41:146–147

Villa IM (1988) Excess Ar in K-rich volcanites: the role of fluids. Rend Soc Ital Miner Petrol 43:95–104

Villa IM (1991) Excess Ar geochemistry in potassic volcanites. Schweiz Mineral Petrog Mitt 71:205–219

Villa IM (1992) Datability of Quaternary volcanic rocks: an $^{40}Ar/^{39}Ar$ perspective on age conflicts in lavas from the Alban Hills, Italy. Eur J Mineral 4:369–383

Villa IM (2001) Radiogenic isotopes in fluid inclusions. Lithos 55:115–124

Villa IM, Grobéty B, Kelley SP, Trigila R, Wieler R (1996) Assessing Ar transport paths and mechanisms for McClure Mountains Hornblende. Contrib Mineral Petrol 126:67–80

Villa IM, Ruggieri G, Puxeddu M (1997) Petrological and geochronological discrimination of two white-mica generations in a granite cored from the Larderello-Travale geothermal field (Italy). Eur J Mineral 9:563–568

Villa IM, Hermann J, Münterer O, Trommsdorff V (2000) $^{39}Ar$-$^{40}Ar$ dating of multiply zoned amphibole generations (Malenco, Italian Alps). Contrib Mineral Petrol 140:363–381

Wartho JA, Kelley SP (2003) $^{40}Ar/^{39}Ar$ ages in mantle xenolith phlogopites: determining the ages of multiple lithospheric mantle events and diatreme ascent rates in southern Africa and Malaita, Solomon Islands. In: Vance D, Müller W, Villa IM (eds) Geochronology: Linking the isotopic record with petrology and textures. Geol Soc London Spec Publ 220: 231–248

Wijbrans JR, Schliestedt M, York D (1990) The tertiary metamorphic evolution of the blueschist terrane of Sifnos, Greece: a study of single mica grains by argon laser probe. Geol Soc Australia Abstracts 27:111

Wulf S, Kraml M, Brauer A, Keller J, Negendank JFW (2004) Tephrochronology of the 100 ka lacustrine sediment record of Lago Grande di Monticchio (southern Italy). Quaternary Internat 122:7–30